European Conference on Optical Communication (ECOC) 2022 © Optica Publishing Group 2022

Fiber Bragg Grating in an Antiresonant Hollow-Core Fiber

Charu Goel(1) and Seongwoo Yoo(1)

(1) The Photonics Institute, School of Electrical and Electronic Engineering, Nanyang Technological University, 50 Nanyang Avenue, Singapore cgoel@ntu.edu.sg

Abstract *We investigate the feasibility of a Fiber Bragg Grating (FBG) in an antiresonant hollow-core fiber by exploiting the enhanced mode-field overlap of the fundamental mode with silica cladding, in the resonant band of wavelengths. The proposed FBG can achieve high reflectivity with an insertion loss of 0.5 dB. ©2022 The Author(s)*

Introduction

Hollow-core fibers (HCFs) have revolutionized the field of fiber optics in the past couple of decades because of the unique advantages offered by propagation of light in air. HCFs exhibit ~30% reduction of latency, orders of magnitude lower nonlinearity and a much higher power-handling capacity, as compared to the standard all-solid fibers [1]. The latest reports based on antiresonant hollow-core fibers (ARHCFs) have demonstrated propagation loss comparable to silica in C and L bands, making them a promising candidate for next generation optical communication systems [2]. To achieve the goal of all-fiber systems based on ARHCFs, it is imperative to develop compatible passive components like wavelength filter [3], polarizer [4], coupler [5], mode-converter [6] etc.

Fiber Bragg grating (FBG) is another critical component for an optical communication system [7]. FBGs are also widely used in sensing applications because of their compact size, high sensitivity, and ease of multiplexing [8]. FBGs work by the principle of coupling of the fundamental mode to the backward propagating mode by virtue of externally induced periodic perturbation of refractive index in the fiber core, over a short length [9]. Due to the excellent confinement of light in the hollow-core of an ARHCF [10] and an extremely low overlap of the fundamental mode field with surrounding silica cladding, it has not yet been possible to develop a fiber Bragg grating in this fiber. In this work, we report a nested ARHCF design, operating in the resonant band of wavelengths, to achieve a high-efficiency FBG with low insertion loss. It is the first design to realise an FBG in a hollow-core fiber. The proposed FBG should find applications in temperature-insensitive environmental sensing [11], gas-filled hollow-core fiber-based laser systems [12], and future optical communication systems based on ARHCFs [13].

Design principles

ARHCFs belong to a special class of HCFs, wherein light guidance can be explained by the principle of antiresonant reflection in waveguides (ARROW) [14] and inhibited coupling of fundamental core mode with lossy modes of the silica cladding [15]. The confinement of light is enhanced by the negative curvature of the core boundary [16]. A typical ARHCF transmission spectrum consists of wavelength bands characterized by high (resonant bands) and low (antiresonant bands) confinement loss (*CL*). The long wavelength edge of the resonant band can be estimated by the condition –

$$\lambda = \frac{2t}{m}\sqrt{(n^2-1)} \quad (1)$$

where t is the wall thickness of the cladding capillaries, n is the refractive index of silica glass, λ is the operating wavelength, m is an integer and hollow core region's refractive index is assumed to be 1. Fig. 1a and 1b show the schematic transverse cross-sections of a single tube lattice ARHCF and a nested ARHCF (NANF) [17] respectively. A nested structure increases the confinement of fundamental mode field to the hollow core region by virtue of two additional dielectric-air interfaces [10]. Here D is the core diameter, t and t_n are the wall thicknesses of the outer and the nested capillaries respectively, and d and d_n are the diameters of the outer and nested capillaries, respectively.

In the antiresonant wavelength band of an ARHCF, the fundamental mode field is well confined to the hollow-core region and as a result

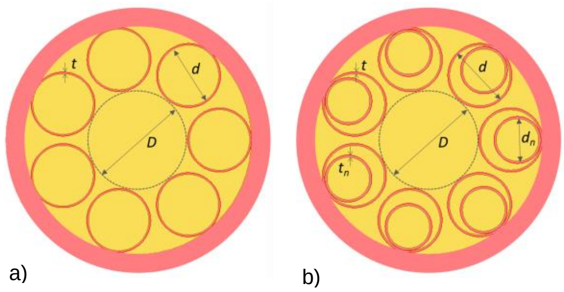

Fig. 1: a) Single ring ARHCF design b) Nested ARHCF (NANF) design with different thickness of outer and nested capillaries. Yellow region: *air*, pink region: *silica*

$<10^{-4}$ fraction of the total optical power lies in the cladding region, leading to minimal overlap of the fundamental mode field with the silica capillaries. To inscribe an FBG in a hollow-core fiber, the periodic perturbation of refractive index can only be induced on the silica cladding. Therefore, the fundamental mode field should have a sizeable overlap with the silica cladding to achieve a significant Bragg reflection. The coupling coefficient κ for contra-directional coupling of the fundamental mode is proportional to the overlap integral of the fundamental mode field with the refractive index perturbation Δn, and is defined by Eqn. 2 [9]. Here E is the transverse electric field of the fundamental mode, ω is the operating angular frequency, ε_0 is the free space permittivity and the refractive index perturbation Δn^2 can be approximated as $2n\Delta n$. Since the refractive index perturbation can be inscribed only on the silica capillaries, $\Delta n = 0$ elsewhere, the surface integral is evaluated numerically only over the capillaries. The length of the FBG required for maximum reflection is given by L = *1/*κ.

$$\kappa = \frac{\omega\varepsilon_0}{4} \iint E^* \Delta n^2 E \, da \qquad (2)$$

The grating period Λ can be evaluated by the standard grating equation, where n_{eff} is the effective refractive index of the fundamental mode:

$$\Lambda = \frac{\lambda}{2n_{eff}} \qquad (3)$$

In pure silica glass, UV phase mask writing technique can produce $\Delta n \sim 5 \times 10^{-4}$ [18], while a femtosecond laser inscription can result in $\Delta n > 1 \times 10^{-3}$ [19].

Results and discussion

We simulated the ARHCFs using full vector finite element method using COMSOL Multiphysics software. The performance of the FBG was optimized for shorter length for practical fabrication and lower insertion loss. We first modelled a single ring ARHCF (Fig. 1a) and assumed core diameter D = 30 µm, t = 0.5 µm and capillary diameter d = 0.6D to ensure effective single mode operation in the widely used 1 µm wavelength region. A uniform refractive index perturbation is assumed for all capillaries, and zero elsewhere. It was found that for λ in the antiresonant band, $\Delta n = 1 \times 10^{-3}$ would necessitate > 1 m long FBG, which is impractical.

The overlap of the mode field with silica cladding increases as one approaches the resonant band of wavelengths, which opens a window of opportunity to achieve higher κ, and hence, shorter FBG. However, as the field spreads out to the cladding, the *CL* also increases. Fig. 2 shows the spectral variation of the required grating length and *CL* in a single ring ARHCF.

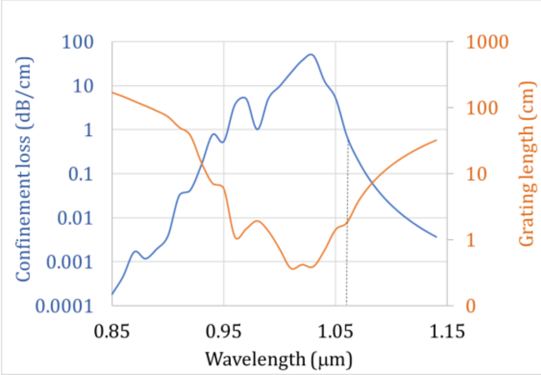

Fig. 2: Spectral variation of confinement loss and grating length for maximum coupling in a single ring ARHCF.

We note from Fig. 2 that the resonant wavelength region from 0.91 µm to 1.11 µm is characterised by a high *CL*. We also note that as we approach the centre of this resonant wavelength band, the required grating length decreases and *CL* follows the reverse trend, and peaks up for wavelengths in the centre of the resonant band. The insertion loss of the FBG will be a product of grating length and the *CL*. The transmission spectrum can be shifted solely by changing the capillary wall thickness *t* (Eq. 1). Hence, one can optimize *t* for the operating wavelength to correspond to low insertion loss and a practical grating length of few centimetres. Data derived from Fig. 2 suggests that the best possible results for an FBG in the considered single ring ARHCF are at 1.06 µm, corresponding to a grating length *L* = 1.8 cm and insertion loss = 1.3 dB. These results are a huge improvement over an FBG designed operating at a wavelength within the antiresonant band, but these numbers can be improved further by taking advantage of state-of-the-art NANF design (Fig. 1b).

We designed a NANF structure to have bi-thickness capillaries such that the operating wavelength corresponds to the resonant band of the outer capillaries, but to the antiresonant band of the nested capillaries. While the outer capillaries weaken the confinement of the fundamental mode field and allow for a sizeable overlap with the silica region, the nested capillaries, corresponding to the antiresonance region, resist the spread of mode field further into the silica jacket. As a result, the overall *CL* is reduced appreciably, and one gets additional design handles to achieve shorter grating length along with lower *CL*. We performed a systematic parametric study over different fiber parameters to achieve the optimized fiber design. Table 1 lists the optimized fiber parameters.

Tab. 1: Fiber parameters of the bi-thickness NANF

Fiber parameter	Symbol	Value (μm)
Core diameter	*D*	30
Diameter of outer capillary	*d*	18
Wall thickness of outer capillary	*t*	0.57
Diameter of nested capillary	d_n	12.7
Wall thickness of nested capillary	t_n	0.65

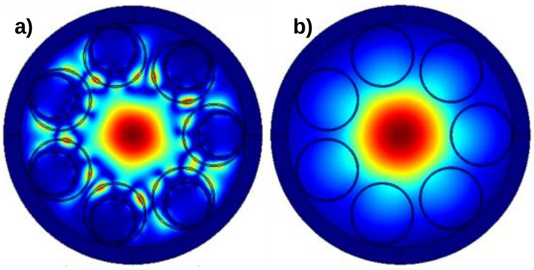

Fig. 3: Fundamental mode field at operating wavelength in a) bi-thickness NANF b) single ring ARHCF

Figs. 3a and 3b respectively show the fundamental mode fields in the optimized bi-thickness NANF and the single ring ARHCF. We note how the fundamental mode is coupled to the outer capillaries in the NANF, while the nested capillaries remain antiresonant. Fig. 4 shows the spectral variation of the FBG length and *CL* in the bi-thickness NANF. The several sharp loss peaks in the spectrum and corresponding peaks in the FBG length are noteworthy here. Each loss peak corresponds to the resonant coupling of the fundamental core mode to discrete cladding modes, which is a typical characteristic of antiresonant fibers [15]. At each of these resonant wavelengths, the effective refractive index of the mode, the spread of the fundamental mode field and the *CL* undergoes a dramatic variation. If the intended fiber device is short (few cm long), then the loss of the device can be designed to be negligible (< 1 dB) even while operating within the resonant band. We have earlier exploited these in-resonant band loss peaks for realising an inline fiber polarizer in a bi-thickness ARHCF and have experimentally demonstrated a compact, low-loss, high-efficiency device [4].

For the designed NANF at λ=1.08 μm, the required grating period is 2.2 μm and the resultant FBG is expected to have a short length of 0.3 cm with a propagation loss of only 0.3 dB.

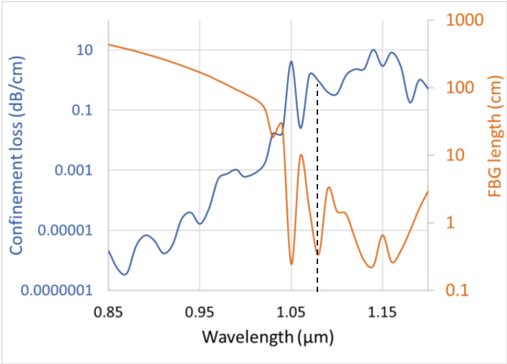

Fig. 4: Spectral variation of confinement loss and grating length for maximum coupling in the bi-thickness NANF.

These values are a significant improvement over a single ring ARHCF.

We also investigated the effect of number of rings in the ARHCF structure on the performance of the FBG. We found that even though increasing the number of rings confines the mode field better and improves the confinement loss, the net overlap with refractive index perturbation increases because of more silica rings. Our simulations reveal that the fraction of total power overlapping with silica rings in the optimized 6-ring NANF (6R-NANF) is 0.8%, while that in a 7R-NANF is 3%. Therefore, a 7R-NANF led to better FBG (shorter length and lower loss) than a 6R NANF. However, increasing the number of rings beyond 7 deteriorates the higher order mode extinction ratio (HOMER) of the fiber [20].

The designed FBG can easily be fusion spliced to a mode-matched standard ARHCF with splice loss as low as < 0.2 dB [4]. The total insertion loss of the FBG (splice loss + propagation loss) is thus expected to be ~0.5 dB. Even though the modal overlap with silica cladding is purposely increased in the proposed FBG, the total fraction of light in the silica cladding is still <5%. Therefore, the hollow-core FBG is expected to have much better thermal insensitivity and power handling capacity as compared to all-solid FBG, where 100% of light is confined to silica.

Conclusions

We present the first design for a hollow-core fiber Bragg grating. The design principles are discussed in detail and the FBG is optimized in terms of practicality of fabrication as well as insertion loss. The simulation results are promising to lead fabrication trials.

Acknowledgements

The authors thank National Research Foundation grant QEP-P4 for providing financial support for this research.

References

[1] Zhixin Liu, Boris Karanov, Lidia Galdino, John R. Hayes, Domaniç Lavery, Kari Clark, Kai Shi, Daniel J. Elson, Benn Charles Thomsen, Marco N. Petrovich, David J. Richardson, Francesco Poletti, Radan Slavík, and Polina Bayvel, "Nonlinearity-Free Coherent Transmission in Hollow-Core Antiresonant Fiber," Journal of Lightwave Technology, vol. 37, pp. 909-916, 2019
DOI: 10.1109/JLT.2018.2883541

[2] *G. T. Jasion, T. D. Bradley, K. Harrington, H. Sakr, Y. Chen, E. N. Fokoua, I. A. Davidson, A. Taranta, J. R. Hayes, D. J. Richardson, and F. Poletti, "Hollow Core NANF with 0.28 dB/km Attenuation in the C and L Bands," in Optical Fiber Communication Conference Postdeadline Papers 2020, paper Th4B.4 (2020).
DOI: 10.1364/OFC.2020.Th4B.4

[3] X. Huang, K. T. Yong, and S. Yoo, "A method to process hollow-core anti-resonant fibers into fiber filters," Fibers, vol. 6, no. 4, p. 89, Aug. 2018
DOI: 10.3390/fib6040089

[4] C. Goel, J. Zang, M. R. A. Hassan, W. Chang, and S. Yoo, "Hollow-Core Fiber Based Inline Polarizer" Paper no. SW4K.5, Conference on Lasers and Electro-optics (CLEO), San Jose, U.S.A. (2022).

[5] X. Huang, J. Ma, D. Tang, and S. Yoo, "Hollow-core air-gap anti-resonant fiber couplers," *Opt. Express*, vol. 25, no. 23, pp. 29296–29306, Nov. 2017.
DOI: 10.1364/OE.25.029296

[6] P. Zhao, H. L. Ho, W. Jin, S. Fan, S. Gao, Y. Wang, and P. Wang, "LP01-LP11 mode conversion in a negative curvature hollow-core fiber by use of a long-period grating," in Asia Communications and Photonics Conference/International Conference on Information Photonics and Optical Communications 2020 (ACP/IPOC), OSA Technical Digest (Optica Publishing Group, 2020), paper M4A.118.
DOI: 10.1364/ACPC.2020.M4A.118

[7] Isabelle Riant, "Fiber Bragg gratings for optical telecommunications", Comptes Rendus Physique, vol. 4, no. 1, pp 41-49, 2003
DOI: 10.1016/S1631-0705(03)00013-6

[8] Chen, J., Liu, B. & Zhang, H., "Review of fiber Bragg grating sensor technology", Frontiers of Optoelectronics in China, vol. 4, pp 204–212, 2011
DOI: 10.1007/s12200-011-0130-4

[9] Raman Kashyap, Chapter 4 - Theory of Fiber Bragg Gratings, Fiber Bragg Gratings (Second Edition), Academic Press, 2010, pp. 119-187, ISBN 9780123725790,
DOI: 10.1016/B978-0-12-372579-0.00004-1

[10] Yingying Wang and Wei Ding, "Confinement loss in hollow-core negative curvature fiber: A multi-layered model," Opt. Express 25, 33122-33133 (2017)
DOI: 10.1364/OE.25.033122

[11] U. S. Mutugala, Fokoua, E.R. Numkam, Y. Chen, T. Bradley, S. R. Sandoghchi, G. T. Jasion, R. Curtis, M. N. Petrovich, F. Poletti, D. J. Richardson and R. Slavík, "Hollow-core fibres for temperature-insensitive fibre optics and its demonstration in an Optoelectronic oscillator", Scientific Reports, vol. 8, article number 18015 (2018).
DOI: 10.1038/s41598-018-36064-1

[12] B. Debord, F. Amrani, L. Vincetti, F. Gérôme and F. Benabid, "Hollow-Core Fiber Technology: The Rising of "Gas Photonics", Fibers 2019, 7(2), 16 (2019)
DOI: 10.3390/fib7020016

[13] F. Poletti and P. Poggiolini, "Potential system impact of low-loss antiresonant hollow core fibers," 45th European Conference on Optical Communication (ECOC 2019), pp. 1-4. 2019.
DOI: 10.1049/cp.2019.1085.

[14] M. A. Duguay, Y. Kokubun, T. L. Koch and L. Pfeiffer L., "Antiresonant reflecting optical waveguides in SiO2-Si multilayer structures," Appl. Phys. Lett. 49(1), 13 (1986)
DOI: 10.1063/1.97085

[15] L. Vincetti and V. Setti, "Waveguiding mechanism in tube lattice fibers," Opt. Express 18, 23133–23146 (2010). DOI: 10.1364/OE.18.023133

[16] Walter Belardi and Jonathan C. Knight, "Effect of core boundary curvature on the confinement losses of hollow antiresonant fibers," Opt. Express 21, 21912-21917 (2013) DOI: 10.1364/OE.21.021912

[17] Francesco Poletti, "Nested antiresonant nodeless hollow core fiber," Opt. Express 22, 23807-23828 (2014)
DOI: 10.1364/OE.22.023807

[18] Jacques Albert, Michael Fokine, and Walter Margulis, "Grating formation in pure silica-core fibers," Optics Letters, vol. 27, pp. 809-811, 2002
DOI: 10.1364/OL.27.000809

[19] Stephen J. Mihailov, Christopher W. Smelser, Dan Grobnic, Robert B. Walker, Ping Lu, Huimin Ding, and James Unruh, "Bragg Gratings Written in All-SiO2 and Ge-Doped Core Fibers With 800-nm Femtosecond Radiation and a Phase Mask," Journal of Lightwave Technology, vol. 22, pp. 94-100, 2004
DOI: 10.1109/JLT.2003.822169

[20] Ge, Aichen, Fanchao Meng, Yanfeng Li, Bowen Liu, and Minglie Hu. 2019. "Higher-Order Mode Suppression in Antiresonant Nodeless Hollow-Core Fibers" Micromachines 10, no. 2: 128.
DOI: 10.3390/mi10020128